Journal of Applied Polymer Science

TiO_2-Oligoaldaramide nanocomposites as efficient core-shell systems for wood preservation

Rosangela Oliva,[1] Antonella Salvini,[1] Giuseppina Di Giulio,[2] Laura Capozzoli,[3] Marco Fioravanti,[2] Cristiana Giordano,[3] Brunella Perito[4]

[1]Dipartimento di Chimica "Ugo Schiff, Università degli Studi di Firenze, Via della Lastruccia 3/13 - 50019 - Sesto Fiorentino (FI), Italy

[2]Dipartimento di Gestione dei Sistemi Agrari, Alimentari e Forestali, Università degli Studi di Firenze, Via San Bonaventura 13 - 50145 - Firenze (FI), Italy

[3]CNR, ICCOM, Electron Miscroscopy Centre "Laura Bonzi" (Ce.M.E.), Via Madonna del Piano 10, 50019 Sesto Fiorentino, Florence, Italy

[4]Dipartimento di Biologia, Università degli Studi di Firenze, Via Madonna del Piano - 6 - 50019 Sesto Fiorentino - (FI), Italy

Correspondence to: A. Salvini (E-mail: antonella.salvini@unifi.it)

ABSTRACT: Homogeneous core-shell systems were obtained with a growth, in controlled steps, of several oligoamides on TiO_2 nanoparticles. Derivatives of natural compounds, such as L-tartaric acid and α,α′-trehalose, were used as diesters in the polycondensation reactions with ethylenediamine. TiO_2 anatase was chosen because of its high photo-activity and its antimicrobial activity. The TiO_2 nanoparticles had been previously activated then functionalized using two different coupling agents, and finally, the TiO_2-oligoamide nanocomposites were synthesized using two synthetic pathways. The final products were characterized by ^{1}H NMR, ^{13}C NMR, FT-IR, and transmission electron microscope. These nanocomposites can show improved properties in comparison with the single components (TiO_2 nanoparticles or oligoamides), which are useful in many fields, such as antimicrobial coatings for surfaces in cultural heritage conservation. A nanocomposite (TiO_2-polyethylenetartaramide) was used for applicative studies, and it has shown a good efficacy against fungal attack by *Trametes versicolor* on wood specimens (*Fagus sylvatica*). © 2015 Wiley Periodicals, Inc. J. Appl. Polym. Sci. **2015**, *132*, 42047.

KEYWORDS: biopolymers and renewable polymers; nanoparticles; nanowires and nanocrystals; polyamides; properties and characterization; synthesis and processing

Received 5 September 2014; accepted 22 January 2015

DOI: 10.1002/app.42047

INTRODUCTION

Several hydroxylated oligoamides have recently been synthesized as water soluble compounds, provided with structural affinity for materials as wood, paper, and natural fibers.[1] Hydroxyl moieties were introduced in the polymeric chain using starting compounds obtained from renewable sources. In particular, natural compounds or derivatives thereof, such as L-tartaric acid, α,α′-trehalose, D(+)-glucose, were used in polycondensation reactions with several diamines.[1,2]

Other hydroxylated oligoamides were synthesized by renewable resources[3–10] and found several industrial applications. A study has been carried out on their use as consolidants[1] for degraded wood, because these compounds show a high affinity for polar materials and similar properties to those of wooden artifacts. The easy biodegradation of natural compounds and their derivatives represents an issue when they are used as consolidants in wood conservation, since their presence can enhance the activity of microorganisms, such as bacteria or fungi. Therefore, to prevent or reduce microorganism growth, a bactericidal agent should be used. In particular, TiO_2 nanocomposites (NCs), if properly irradiated, show antimicrobial properties which can be exploited to avoid fungal attacks on wooden surfaces. In fact, the photocatalytic efficiency of TiO_2 nanoparticles (NPs) was observed against attacks of bacteria,[11–20] mold,[20] and fungi.[13,17,21–23]

Anatase is a metastable crystal structure of TiO_2[24] which has a better stability than the other metastable form (brookite). The rutile form is the most stable structure, but anatase TiO_2 shows a higher photoactivity compared to the rutile form, in agreement with the band-gap energy between the valence band and the conduction band, which is 3.00 eV for rutile and 3.23 eV

Table I. Code of Synthetized Products

Code products		Reagents
FNP	FNP.1	TiO_2- [3-(2-aminoethylamino)propyl] trimethoxysilane (AEAPTMS)
	FNP.2	TiO_2- (3-aminopropyl)trimethoxysilane (APTMS)
FNPE	FNPE.1	FNP.1 + dimethyl L-tartrate
	FNPE.2	FNP.1 + dimethyl α,α′-trehaluronate
	FNPE.3	FNP.2 + dimethyl L-tartrate
	FNPE.4	FNP.2 + dimethyl α,α′-trehaluronate
FNPO	FNPO.1	FNP.1 + dimethyl L-tartrate + 1,2-ethylendiamine
	FNPO.2	FNP.1 + dimethyl α,α′-trehaluronate + 1,2-ethylendiamine
	FNPO.3	FNP.2 + dimethyl L-tartrate + 1,2-ethylendiamine
	FNPO.4	FNP.2 + dimethyl α,α′-trehaluronate + 1,2-ethylendiamine
FNPEO	FNPEO.1	FNPE.1 + dimethyl L-tartrate + 1,2-ethylendiamine
	FNPEO.2	FNPE.2 + dimethyl α,α′-trehaluronate + 1,2-ethylendiamine
	FNPEO.3	FNPE.3 + dimethyl L-tartrate + 1,2-ethylendiamine
	FNPEO.4	FNPE.4 + dimethyl α,α′-trehaluronate + 1,2-ethylendiamine

for anatase.[25] Consequently, radiation with wavelength <387 nm can selectively excite TiO_2 in anatase form, a behavior of great interest for several applications.

During the past decade, new materials with special and particular properties were obtained combining organic polymers and inorganic materials. Furthermore, since toxicity problems, due to the presence of free nanoparticles,[26,27] have recently been highlighted, the additional presence of a polymeric compound seems important to reduce the mobility[28] of the nanoparticles and their negative effects.

Polymer-based NCs were produced by dispersing nanoparticles in a polymeric formulation. However, the formation of agglomerates and aggregates of nanoparticles deteriorates the mechanical properties and reduces the optical transparency of polymer-based NCs.[29] Many authors have been studying surface modifications of inorganic nanoparticles using organic reagents, with the purpose of reducing agglomerations and increasing the compatibility between inorganic particles and polymer matrixes[29–31] so as to yield more homogeneous composites. In particular, nanoparticle-polymer composites were obtained by grafting end-functionalized polymers to NPs[32] or by grafting polymers from NPs with in situ monomer polymerization.[29,33]

Several examples of TiO_2-polymer composites have been described in the literature, such as TiO_2-poly(styrene-divinylbenzene)/maleic anhydride,[34] TiO_2-polypirrole,[35] TiO_2-PMMA,[36] TiO_2/poly (amide-imide),[37,38] TiO_2/P(St-*co*-DVB)-MAA,[39] TiO_2/polystyrene,[40] $TiO_2(SiO_2)$/PVDF/PMMA,[41] TiO_2/(VAc-BuA),[42] TiO_2/PET.[43]

In this work, NCs (NPs-Oligoamide), containing hydroxylated oligomers derived from renewable sources and covalently bonded to anatase TiO_2 nanoparticles, were synthesized with the purpose of obtaining new formulations with antimicrobial properties to be used afterward on wooden surfaces. The simultaneous presence of anatase TiO_2 nanoparticles could improve the properties of these oligoamides, when used for surface treatment of wood, paper, leather, or natural fibers. The hydroxylated oligoamides were synthesized on TiO_2 nanoparticles through multi-step reactions and with modified versions of procedures which had already been used for the synthesis of corresponding hydroxylated oligoamides.[1] The products were characterized by ^1H NMR, ^{13}C NMR, FT-IR spectroscopies, dynamic light scattering (DLS), and by transmission electron microscope (TEM).

Applicative studies were carried out to evaluate the efficacy of one of the synthesized compounds against attacks of microorganisms on wood specimens.

EXPERIMENTAL

Materials

L-tartaric acid, boric acid, (diacetoxyiodo)benzene (BAIB), Amberlite IR-120H, ethylenediamine, 2,2,6,6-Tetramethylpiperidine-1-oxyl, 1,4-dioxane, methanol, [3-(2-aminoethylamino)propyl]trimethoxysilane (AEAPTMS), (3-aminopropyl)trimethoxysilane (APTMS), Titanium(IV) oxide (powder, $d < 25$ nm, anatase), α,α′-trehalose, and D_2O were purchased from Aldrich. Triethylamine was purchased from Carlo Erba.

Amberlite IR-120H resin was activated by washing with methanol (3 × 10 mL) and left overnight in methanol (10 mL). All chemicals were reagent grade and were used without further purification.

Microorganism and Growth Conditions

Trametes versicolor strain MB52, purchased from the Austrian Center of Biological Resources and Applied Mycology, was used as test organism in this study. To test wood specimens susceptibility to fungal attack, a cell suspension of *T. versicolor* was spread on Malt Extract Agar (MEA, OXOID) plates and incubated at 30°C for 4 weeks to obtain a thick mycelium.

Preparation of Wood Specimens

Sixteen samples were prepared from European beech (*Fagus sylvatica L.*), a wood specie that is well known for its low natural durability and high susceptibility to Fungi and Bacteria, which make it one of the most suitable one to test the performances of antimicrobial products. Wood specimens were prepared using material free of any previous biological alteration, and cutting the wood with the longitudinal faces parallel to the grain, up to a final size of 10 × 20 × 2 mm. Prior to the treatment the wood samples were equilibrated at 20°C and 65% relative humidity (RH) inside dryers which contained xylene as inhibitor of Fungal activity.

Instruments

^1H NMR and ^{13}C NMR spectra were recorded with a Varian Mercury Plus 400 spectrometer and a Varian VXR 200

Table II. FT-IR Spectral Data (KBr Pellets)

Product	N-H and O-H stretching	C-H stretching	C=O stretching (Ester)	C=O stretching (Amide I)	N-H bending (Amide II)	C-H bending	C-N stretching	Si-O stretching	C-O stretching	Ti-O-Si stretching	Ti-O stretching
FNPE.1 FNPE.3	3342 (vs[b], broad)	2952 (w[b]) 2880 (w)	1738 (s[b])	N.D.[c]	N.D.[c]	1464 (w)	1353 (w)	1127 (vs) 1080 (vs)	1127 (vs) 1080 (vs)	904 (w)	620 (vs)
FNPE.2 FNPE.4	3343 (vs, broad)	2932 (w)	1730 (s)	N.D.[c]	N.D.[c]	1411 (w)	1353 (w)	1151 (s) 1070 (s)	1151 (vs) 1108 (vs) 1070 (vs) 1027 (vs)	912 (w)	620 (vs)
FNPO.1[a] FNPO.3[a] FNPEO.1[a] FNPEO.3[a]	3348 (vs, broad)	2933 (w) 2873 (w)	1730 (w)	1660 (vs)	1537 (s)	1436 (w)	1353 (w)	1134 (w) 1072 (w)	1134 (w) 1072 (w)	915 (w)	620 (vs)
FNPO.2[a] FNPO.4[a] FNPEO.2[a] FNPEO.4[a]	3416 (vs, broad)	2935 (w)	1730 (w)	1660 (vs)	1540 (s)	1415 (w)	1353 (w)	1150 (w) 1066 (w)	1150 (s) 1107 (s) 1066 (s) 1028 (s)	942 (w)	620 (vs)

[a] Spectrum recorded on the mixture of soluble (*A*) and insoluble (*B*) fractions.
[b] vs: very strong; s: strong; w: weak.
[c] N.D.: not observed separately for the presence of other overlapped bands (N—H amine bending, H—OH bending).

Table III. ^{1}H NMR Spectral Data (400 MHz, δ, ppm, D_2O)

	Silyl derivate moiety				
Product	Si-C**H**$_2$	Si-CH$_2$-C**H**$_2$	Si-(CH$_2$)$_2$-C**H**$_2$-NH-C**H**$_2$	Si-(CH$_2$)-C**H**$_2$-NHCO	NH-CH$_2$-C**H**$_2$-NHCO
FNPE.1	0.73	1.81	3.00-3.28	-	3.60
FNPE.2[a]	0.68	1.75	3.01-3.26	-	3.60
FNPE.3[a]	0.77	1.81	-	3.05	-
FNPE.4[a]	0.77	1.83	-	3.10	-
FNPO.1[b]	0.70	1.73	2.90-3.15	-	3.40-3.60
FNPO.2[b]	0.67	1.75	3.00-3.20	-	3.40-3.60
FNPO.3[b]	0.70	1.79	-	3.00-3.15	-
FNPO.4[b]	0.67	1.74	-	3.00	-
FNPEO.1[b]	0,72	1,77	3.07-3.20	-	3.40-3.60
FNPEO.2[b]	0.69	1.74	3.00-3.15	-	3.40-4.60
FNPEO.3[b]	0.71	1.79	-	3.00	-
FNPEO.4[b]	0.76	1.81	-	3.00-3.20	-

[a] Spectra recorded at 200 MHz.
[b] Spectra recorded on the soluble fraction of nanocomposite.

spectrometer, working at 399.921 MHz and 199.985 MHz, respectively. All spectra are reported in ppm and referred to TMS as internal standard. Spectra elaboration was performed with the software Mestre-C 4.3.2.0.

FT-IR spectra were recorded with a Shimadzu FT-IR-8400S model and elaborated with the Spectrum v.3.0202. Solutions were analyzed using KBr or CaF_2 round cell windows, after deposition and evaporation of solvent. Spectra of solid samples were recorded as KBr pellets.

DLS measurements were carried out by means of a BI-90Plus light scattering apparatus from Brookhaven Instruments. The autocorrelation functions recorded for each sample are the result of an average of 10 individual measurements and data were analyzed according to the CONTIN algorithm to provide the size distribution of scattering objects. Diluted dispersions were investigated in the conventional geometry (at a scattering angle of 90°). Nondiluted dispersions, due to their opacity, cannot be investigated in such geometry; therefore, they were

Table IV. ^{1}H NMR Spectral Data (400 MHz, δ, ppm, D_2O)

	Diamine moiety		Dicarboxylic moiety								
Product	C**H**$_2$NHCO	C**H**$_2$NH$_2$	OCH$_3$	C**H**-OH near ester group	C**H**-OH near amide group	H-1	H-2	H-3	H-4	H-5	H-5 end chain
FNPE.1	-	-	3.82	4.66	4.40	-	-	-	-	-	-
FNPE.2[a]	-	-	3.80	-	-	5.19	3.69	3.84	3.60	4.00-4.20	4.40
FNPE.3[a]	-	-	3.84	4.68	4.42	-	-	-	-	-	-
FNPE.4[a]	-	-	3.80	-	-	5.19	3.69	3.82	3.58	4.00-4.17	4.40
FNPO.1[b]	3.40-3.60	2.90-3.15	-	-	4.57	-	-	-	-	-	-
FNPO.2[b]	3.40-3.60	3.00-3.20	-	-	-	5.18	3.67	3.84	3.53	4.00-4.25	-
FNPO.3[b]	3.40-3.60	3.03-3.15	-	-	4.57	-	-	-	-	-	-
FNPO.4[b]	3.40-3.60	3.16	3.80	-	-	5.18	3.68	3.85	3.54	3.90-4.20	4.38
FNPEO.1[b]	3.40-3.60	3.07-3.20	-	-	4.58	-	-	-	-	-	-
FNPEO.2[b]	3.40-4.60	3.00-3.15	-	-	-	5.23	3.70	3.86	3.58	4.07-4.27	-
FNPEO.3[b]	3.46	3.20	-	-	4.57	-	-	-	-	-	-
FNPEO.4[b]	3.54	3.00-3.20	-	-	-	5.23	3.73	3.89	3.59	4.10-4.30	-

[a] Spectra recorded at 200 MHz.
[b] Spectra recorded on the soluble fraction of nanocomposite.

Table V. Syntheses of Nanocomposites

Product	Molar ratio[a]	Yield *A*+ *B* (%)	DP[b] (*A*)
FNPO_1	1 : 3 : 2	67.3	2
	1 : 4 : 3	72.5	3
	1 : 10 : 9	75.0	6
FNPO_2	1 : 3 : 2	57.0	2
FNPO_3	1 : 3 : 2	63.0	3
FNPO_4	1 : 3 : 2	31.0	2
FNPEO_1	1 :5 : 6	66.0	8
	1 : 9 : 10	74.0	12
FNPEO_2	1 : 5 : 6	77.8	9
FNPEO_3	1 : 5 : 6	74.6	17
FNPEO_4	1 : 2 : 3	70.4	14

[a] Molar ratio FNPE (or FNP) : diester : diamine.
[b] DP = degree of polymerization of the soluble fraction (*A*).

investigated by means of a Fiber Optic Quasi-Elastic Light Scattering (FOQELS) accessory (at a scattering angle of 135°).

TEM analyses were performed on TEM Philips CM 12, equipped with an Olympus Megaview G2 camera and using an accelerating voltage of 100 kV. Samples were prepared by depositing a drop of dispersion of the sample on carbon film of 200 mesh Cu grid.

Exposure to UV radiation was carried out using a Spectroline Lamp, Model ENF-260C/FE, with an emission in UV-A range at wavelength of 365 nm (tube of 6 W).

The colorimetric analyses were performed using a CM-2600d Konica-Minolta portable spectrophotometer equipped with the integrative sphere inside the apparatus and a Xenon lamp to pulse the light on the sample surface. The measurement aperture is 3 mm, and light is reflected from the surface at an angle of 8°. Color coordinates are based on CIEL*a*b* system using an illuminant D65 with an observer angle of 10°. Sample surface was observed with a Dino-Lite Pro Portable Digital Microscope with 1.3 megapixel image sensor. The microscope is equipped with polarized light (useful with reflective objects) and magnification up to 200×.

Synthesis of Dimethyl Esters

Dimethyl L-tartrate, α,α′-trehaluronic acid and dimethyl α,α′-trehaluronate were synthesized according to literature methods.[1]

TiO_2 Activation

TiO_2 (1.6 g, 0.02 mol) nanoparticles were dispersed in HNO_3 (2M). The dispersion was placed in a flask fitted with a reflux condenser and heated at 95°C for 8 h. The mixture was cooled and centrifuged; then the solid was dispersed in Milli-Q water (35 mL).

Functionalized Nanoparticle Syntheses

Functionalized nanoparticles (FNP) were synthesized using two different silylating agents, AEAPTMS and APTMS, obtaining respectively, FNP.1 and FNP.2, as reported in Table I.

Synthetic Procedure. Into a Soviral® tube, the silylating agent (1.6 mmol) was added under continuous stirring to 3.80 mL of methanol. Then, a water dispersion of TiO_2 nanoparticles at 4.5% (3.75 mmol) was added and the blend was sonicated for 30 min. The mixture was heated at 40°C for 15 h under dry nitrogen atmosphere. After having cooled to room temperature, a sample of the dispersion of nanoparticles (0.5 mL) was recovered and solvent and volatile compounds were distilled at reduced pressure and at 40°C. The resulting white solid was washed with chloroform, recovered by centrifugation (5 min at 2800 rpm), then dried in vacuum at room temperature (yield ≈ 90%). The obtained solid was analyzed by FT-IR spectroscopy and after dispersion in D_2O by ^1H and ^{13}C NMR spectroscopies.

FNP.1: ^1H NMR (D_2O, 400 MHz): 0.70 ppm (m, 2H, —Si—C**H**$_2$—); 1.73 ppm (m, 2H, —Si—CH_2—C**H**$_2$—); 2.93 ppm (m, 6H, —Si—$(CH_2)_2$—C**H**$_2$—NH—(C**H**$_2$)$_2$—NH_2). ^{13}C NMR (D_2O, 100 MHz): 9.8 ppm (—Si—**C**H_2—); 21.0 ppm (—Si—CH_2—**C**H_2—); 38.1 ppm (—Si—$(CH_2)_3$NH—CH_2—**C**H_2—NH_2); 48.8 ppm (—Si— $(CH_2)_3$NH—**C**H_2—CH_2—NH_2); 50.6 ppm (—Si—$(CH_2)_2$—**C**H_2—NH—). FTIR (KBr pellets): peaks at 3246 (s, broad,

Table VI. ^{13}C NMR Spectral Data (100 MHz, δ, ppm, D_2O)

	Silyl derivate moiety				
Products	Si-**C**H_2	Si-CH_2-**C**H_2	Si-$(CH_2)_2$-**C**H_2-NH	NH-**C**H_2-CH_2-NH	NH-CH_2-**C**H_2-NHCO Si-$(CH_2)_2$-**C**H_2-NHCO
FNPO.1 and FNPEO.1[a]	9.3	20.6	50.3	46.9	38.5-39.4
FNPO.3 and FNPEO.3[a]	8.8	20.8	-	-	37.9-39.4
FNPO.2 and FNPEO.2[a]	8.7	19.6	49.9	46.6	38.4-39.0
FNPO.4 and FNPEO.4[a, b]	N.D.[c]	N.D.[c]	-	-	N.D.[c]

[a] Soluble fraction of nanocomposite.
[b] Signals attributable to the coupling agent are not visible with increasing molecular weight of the polymers.
[c] N.D.: not determined.

Table VII. ^{13}C NMR Spectral Data (100 MHz, δ, ppm, D_2O)

	Diamine moiety		Dicarboxylic moiety							
Products	**C**H_2NH amide	**C**H_2NH_2	-OCH_3	**C**H-OH	C-1	C-2	C-3	C-4	C-5	C=O
FNPO.1 and FNPEO.1[a]	38.5-39.4	N.D.[b]	-	72.3-73.8	-	-	-	-	-	174.0-174.8
FNPO.3 and FNPEO.3[a]	37.9-39.4	N.D.[b]	-	72.3-73.8	-	-	-	-	-	174.0-174.4
FNPO.2 and FNPEO.2[a]	38.4-39.0	N.D.[b]	-	-	93.4-94.3	70.4	71.9	71.6	71.9	171.2-176.3
FNPO.4 and FNPEO.4[a]	36.7-39.0	41.6	53.0	-	93.5-94.6	70.4	72.0	71.3	71.6	171.2-176.3

[a] Soluble fraction of nanocomposite.
[b] N.D.: not determined.

N—H and O—H stretching), 2924 (w, C—H asymmetric stretching), 2870 (w, C—H symmetric stretching), 1596 (s, N—H bending), 1457 (w, C—H bending), 1353 (m, C—N stretching), 1115 (s, Si—O asymmetric stretching), 1031 (s, Si—O asymmetric stretching), 933 (w, Ti—O—Si stretching), 620 (vs, Ti—O stretching) cm^{-1}.

FNP.2: ^1H NMR (D_2O, 400 MHz): 0.66 ppm (m, 2H, —Si—C**H**$_2$—); 1.76 ppm (m, 2H, —Si—CH_2—C**H**$_2$—); 2.98 ppm (m, 2H, —Si—CH_2—CH_2—C**H**$_2$—NH_2). ^{13}C NMR (D_2O, 100 MHz): 9.5 ppm (—Si—**C**H_2—); 21.6 ppm (—Si—CH_2—**C**H_2—); 42.0 ppm (—Si— $(CH_2)_2$—**C**H_2—NH_2). FTIR (KBr pellets): peaks at 3343 (s, broad, N—H and O—H stretching), 2924 (w, C—H asymmetric stretching), 2880 (w, C—H symmetric stretching), 1595 (s, N—H bending), 1457 (w, C—H bending), 1353 (m, C—N stretching), 1120 (s, Si—O asymmetric stretching), 1033 (s, Si—O asymmetric stretching), 945 (w, Ti—O—Si stretching), 620 (vs, Ti—O stretching) cm^{-1}.

Amide Syntheses by Reaction of FNP and Dimethyl Ester (FNPE)

The amides were obtained by reacting the FNP (FNP.1 or FNP.2) with dimethyl ester (dimethyl L-tartrate or dimethyl α,α′-trehaluronate); the respective products were denoted as shown in Table I.

Synthetic Procedure. Into a Soviral® tube, a methanol solution (2.5 mL) of dimethyl ester (1.06 mmol) was added under continuous stirring to a FNP.1 or FNP.2 dispersion (0.53 mmol). Triethylamine (0.14 mmol) was then added and the mixture was heated at 80°C for 24 h under dry nitrogen atmosphere. After having cooled to room temperature, solvent and volatile compounds were distilled under reduced pressure and at 40°C. The resulting solid (white for tartrate derivative or amber for trehaluronic derivative) was washed with methanol and centrifuged (5 min at 2800 rpm). The residual solid was dried in vacuum at room temperature (yield ≈ 85%), analyzed by FT-IR (Table II) spectroscopy and, after dispersion in D_2O, by ^1H NMR (Tables III and IV) spectroscopy.

Oligoamide Syntheses by Polymerization of FNPE or FNP with Dimethyl Ester and Diamine (FNPO or FNPEO)

Oligoamides were obtained by polymerization of FNP (or FNPE) with dimethyl ester (dimethyl L-tartrate or dimethyl α,α′-trehaluronate) and diamine (ethylenediamine) in equimolar amounts (see Table V). The respective products were denoted as shown in Table I.

Synthetic Procedure to Obtain FNPO. In a Soviral® tube, a methanol solution (1.8 mL) of dimethyl ester (1 mmol) was added under continuous stirring to FNP (0.3 mmol). Then, a methanol solution (1.25 mL) of 1,2-ethylendiamine (0.7 mmol) and triethylamine (0.27 mmol) was added and the mixture was heated at 80°C for 24 h (Table V) under dry nitrogen atmosphere. After having cooled to room temperature, solvent and volatile compounds were distilled under reduced pressure and at 40°C. The solid was washed with methanol and centrifuged (5 min at 2800 rpm) and the resulting solid was dried at room

Table VIII. Treatment of Samples

Sample	Nanocomposite	Exposure	Sample	Nanocomposite	Exposure
1	FNPO.1	Light	9	-	Light
2	FNPO.1	Light	10	-	Light
3	FNPO.1	Light	11	-	Light
4	FNPO.1	Light	12	-	Light
5	FNPO.1	Dark	13	-	Dark
6	FNPO.1	Dark	14	-	Dark
7	FNPO.1	Dark	15	-	Dark
8	FNPO.1	Dark	16	-	Dark

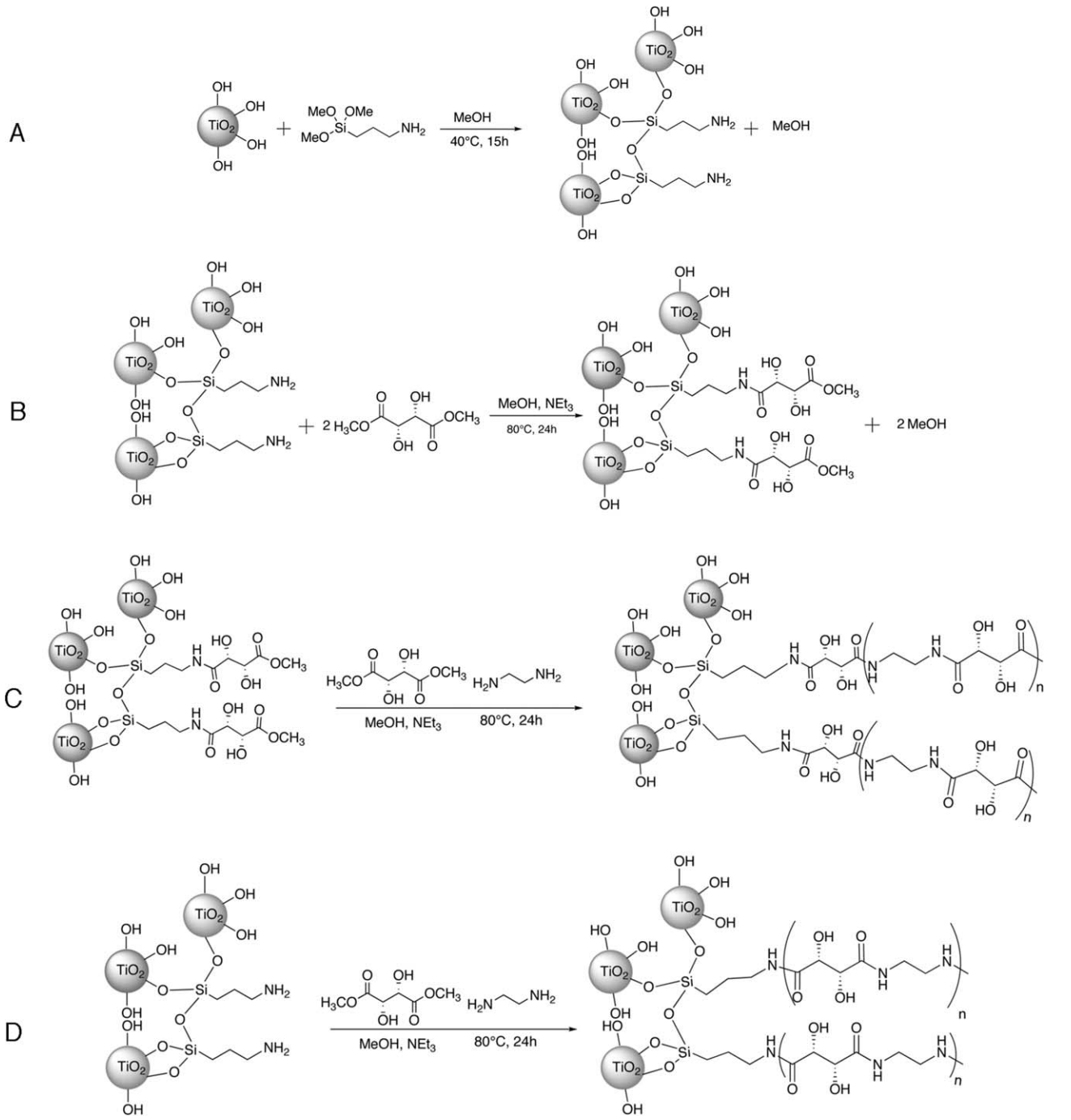

Figure 1. Synthesis of FNP (A), FNPE (B), FNPEO (C), and FNPO (D).

temperature. The solid product (50 mg) was suspended in D_2O (1 mL) in a vial. After centrifugation (1 h at 2800 rpm), a soluble fraction ($A \approx$ 50–60%) in D_2O and an insoluble one ($B \approx$ 40–50%) were obtained. The soluble fraction was analyzed with FT-IR (Table II), ^{1}H NMR (Table III and IV), and ^{13}C NMR (Tables VI and VII) spectroscopies; the insoluble fraction was analyzed with FT-IR spectroscopy (Table II).

Synthetic Procedure to Obtain FNPEO. In a Sovirel® tube, a methanol solution (1.25 mL) of dimethyl ester (0.7 mmol) was added under continuous stirring to FNPE (0.3 mmol). Then, a methanol solution (1.8 mL) of 1,2-ethylendiamine (1 mmol) and triethylamine (0.27 mmol) was added and the mixture was heated at 80°C for 24 h (Table V) under dry nitrogen atmosphere. The work-up was carried out operating as above.

Wood Sample Treatment

The water dispersion of TiO_2-polyethylenetartaramide, containing 460 mg of product [FNPO.1 (1 : 4 : 3)] in 10 mL of water, was used for applications on the wood specimens.

The NC dispersion (6 mL) was applied on all faces of the samples 1–8 using a brush (three applications/day for 7 days), whereas the samples 9–16 were not treated with the NCs. All

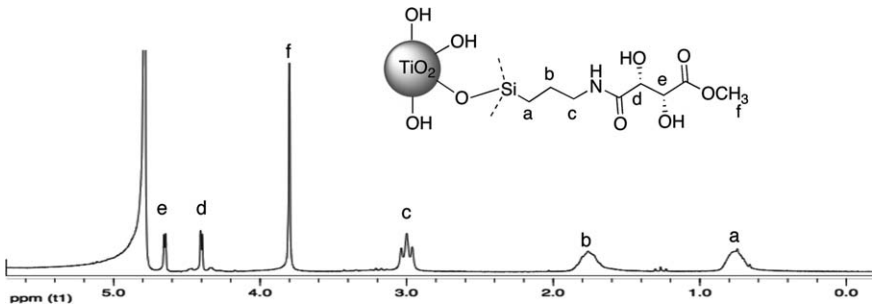

Figure 2. ^{1}H NMR spectrum of FNPE.3 (recorded at 200 MHz).

samples were kept at 65% RH and 20°C in a sterile environment (dried with xylene) until the treatment with the white-rot decay fungus *T. versicolor*. The samples were placed on a sterile small net on *T. versicolor* cultures in Petri dishes (four samples per dish). Half of the samples were exposed to UV light for 3 weeks while the other ones were kept in the dark (Table VIII). For each sample, four repetitions were tested. All the equivalent samples (e.g., samples 1–4) were placed on different Petri dishes to have a better reproducibility.

At the same time, the NC dispersion used in wood sample treatments was deposed on a glass plate and exposed to UV light for 3 weeks. An analogous test was performed with a mixture of the corresponding oligoamide and TiO_2. After 3 weeks, products were recovered from glass plates and analyzed by FT-IR and ^{1}H NMR.

RESULTS AND DISCUSSION

NCs Design

The antimicrobial activity of the titanium dioxide can be extremely relevant to wood conservation, especially when an organic consolidant has to be used. With the purpose of preventing microorganism growth on wooden surfaces, NCs with hydroxylated oligoamides, bonded to TiO_2 anatase, were designed. In fact, oligo-L-tartaramides and oligo-α,α′-thehaluronamides were tested as consolidants for waterlogged archaeological wood, obtaining interesting results.[1] The NC synthetic procedures, similar to that used for the oligoamides,[1] were optimized by testing several multi-step reactions to limit the formation of free oligomer chains. Different products were synthesized to optimize the synthesis procedures and to analyze the influence of different reagents on the synthesis results. In particular, TiO_2 nanoparticles were activated in acidic conditions and then functionalized using silane coupling agents, such as AEAPTMS and APTMS, to introduce an amino group, obtaining, respectively, FNP.1 and FNP.2. Then, the reactivity of FNP with two different dimethyl esters (dimethyl L-tartrate or dimethyl α,α′-trehaluronate) was tested, obtaining FNPE.1, FNPE.2, FNPE.3, and FNPE.4 which contain an ester as the end group of the FNP. Using this approach, it was possible to characterize the first intermediate in the oligoamide synthesis to confirm the reaction between FNP and dimethyl ester. Lastly, to verify the same behavior for FNP containing amino or ester as end group, the oligoamide NCs were synthesized using two different procedures. Indeed, polycondensation reactions with diamines and dimethyl ester were performed using directly FNP derivatives or, after their preliminary reaction with dimethyl ester, using FNPE derivatives.

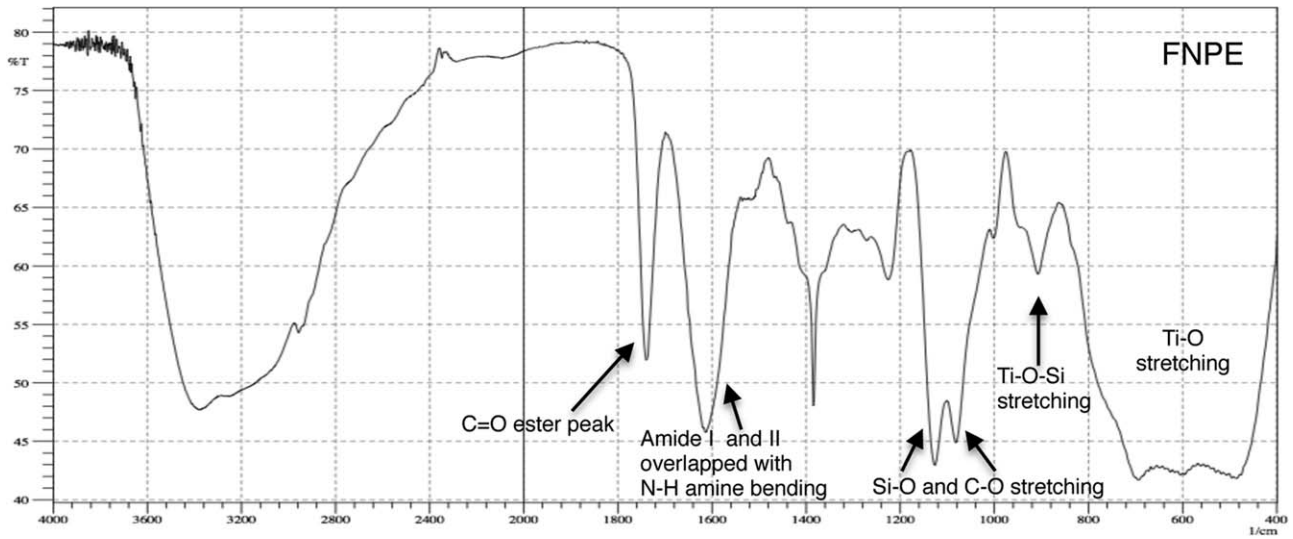

Figure 3. FT-IR spectrum of FNPE.1.

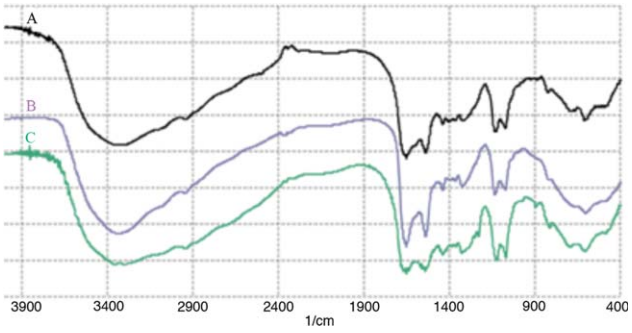

Figure 4. FT-IR spectra comparison between soluble fraction (*A*), insoluble fraction (*B*), and the not separated fractions ($C = A + B$) of the FNPO.1 nanocomposite. [Color figure can be viewed in the online issue, which is available at wileyonlinelibrary.com.]

Synthesis and Characterization of NCs

1. ***TiO_2 activation***: The activation process of TiO_2 was necessary to obtain TiO_2 nanoparticles with exposed Ti—OH groups on the surface layers. The treatment was carried out with HNO_3 (2*M*). The solid, recovered by centrifugation, gave a stable aqueous dispersion (4.5%).
2. ***FNP syntheses***: Amino groups were introduced onto TiO_2 nanoparticles by a reaction between hydroxyl groups and a silylating coupling agent. A water dispersion of NPs (4.5%) was added to the coupling agent diluted in methanol; the mixture was sonicated for 30′, yielding a stable, white dispersion. Two silylating agents, AEAPTMS and APTMS, were used to functionalize the TiO_2 nanoparticles [Figure 1(A)].

   Formation of covalent Si—O—Ti bond was confirmed by the change in chemical shifts of the signals related to AEAPTMS from 0.45 ppm (Si—C***H***$_2$), 1.51 ppm (Si—CH_2C***H***$_2$), and 2.66 ppm (Si—CH_2CH_2C***H***$_2$NH—C***H***$_2C$***H***$_2NH_2$) to 0.70, 1.73, and 2.93 ppm, respectively; analogously, the proton signals of APTMS were shifted from 0.54 ppm (Si—C***H***$_2$), 1.58 ppm (Si—CH_2C***H***$_2$), and 2.70 ppm (Si—CH_2CH_2C***H***$_2NH_2$) to 0.66, 1.76, and 2.98 ppm, respectively.
3. ***Amide syntheses on TiO_2 (FNPE)***: The end group of the FNP was modified by a reaction between FNP dispersion

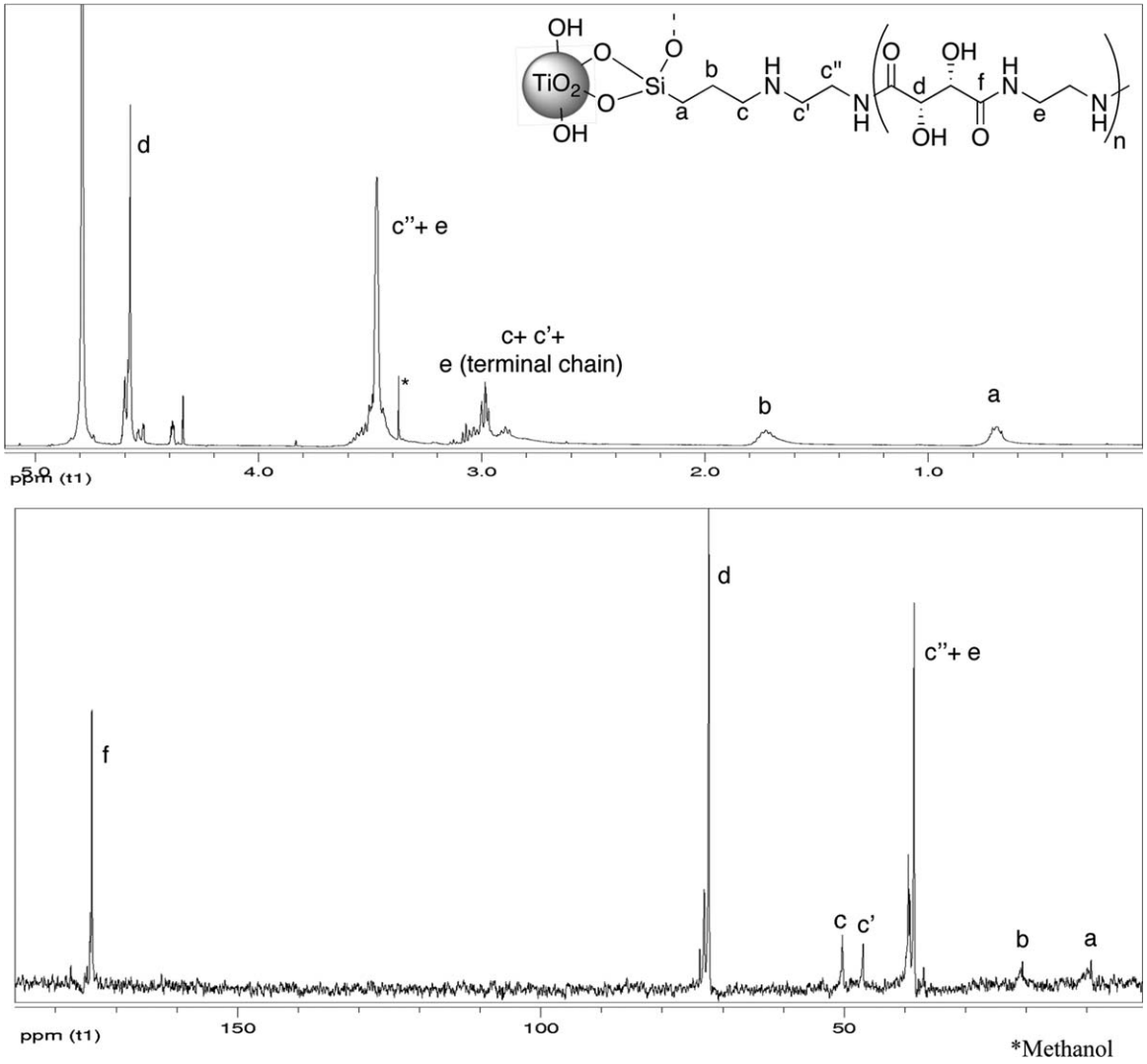

Figure 5. ^1H and ^{13}C NMR spectra of FNPO.1 (1 : 4 : 3).

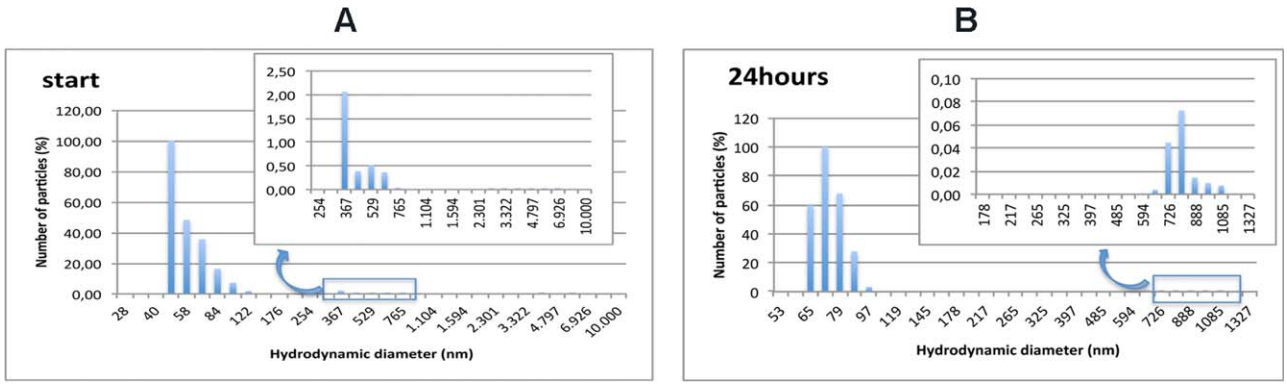

Figure 6. DLS of water dispersion of FNPO.1 (1 : 4 : 3). A: $t = 0$, B: $t = 24$ h. [Color figure can be viewed in the online issue, which is available at wileyonlinelibrary.com.]

and dimethyl ester obtaining an amido compound with an ester as end group [Figure 1(B)].

The molar ratio diester/FNP was set equal to two to avoid the formation of nonreactive products, where both the terminal groups of dimethyl ester have reacted. Successful outcome of the synthesis was confirmed by the ^{1}H NMR spectrum. In fact, the signals of silyl derivative at 0.77 ppm (a), 1.81 ppm (b) and 3.05 ppm (c), the signal (f) of the terminal ester group at 3.84 ppm, the signal (d) of the C**H**—OH group near amide at 4.42 ppm, and the signal (e) of the C**H**—OH group near ester at 4.68 ppm were present in the spectrum (Figure 2). Furthermore, the band attributable to the ester group was present in the FT-IR spectrum. The amide I and II bands could not be observed separately due to the presence of other overlapped bands. Indeed, a band attributable to N—H amine bending is present near 1600 cm^{-1} for FNPE.1 (Figure 3) and FNPE.2, whereas there could be H—OH bending, probably due to coordinated water, for all FNPE products. Several attempts to reduce water presence in these samples were unsuccessful.

4. ***Oligoamide syntheses on TiO_2:*** the polycondensation reaction between FNP, dimethyl ester and diamine [Figure 1(C,D)], was carried out following the procedure previously reported for analogous oligoamides,[1] but with shorter reaction times. The syntheses were performed carried out using different molar ratios diester/diamine and FNP (or FNPE), as reported in Table V.

After the work-up, the solid obtained for each NC was extracted in water, so as to observe the presence of free or bonded oligoamides. The dispersion was stable; however, by centrifugation for 1 h at 2800 rpm, a soluble fraction ($A \approx 50$–60%) and an insoluble one ($B \approx 40$–50%) were separated and their FT-IR spectra were compared (Figure 4). Both fractions showed the same set of signals. However, in the FT-IR spectrum of the soluble fraction [Figure 4(A)], amide signals (1660 and 1540 cm^{-1}) were stronger compared to the characteristic band, due to the TiO_2 nanoparticles (620 cm^{-1}), while the opposite was observed in the insoluble fraction [Figure 4(B)]. Therefore, the NCs were found in both fractions: in the soluble fraction, NCs with longer oligomeric chains were probably present along with oligomeric free chains. All samples showed in the FT-IR spectra the same differences between the two fractions.

The soluble fraction was also analyzed by NMR spectroscopy to have a complete chemical characterization. In Figure 5, ^{1}H and ^{13}C NMR spectra of the soluble fraction (sample FNPO.1) are reported.

The degree of polymerization (DP) of the oligomers found in the soluble fraction, free and bonded to TiO_2, was determined from the integral of signals in the ^{1}H NMR spectrum.

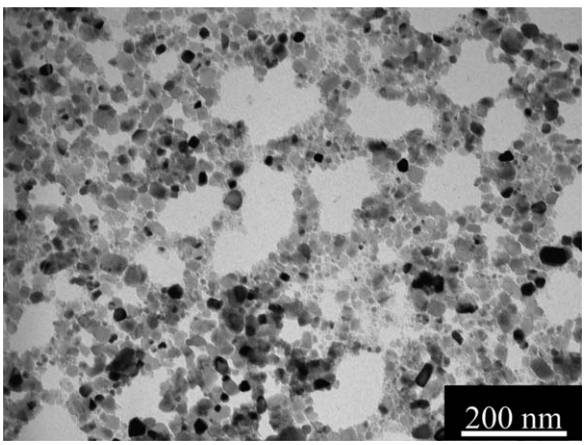

Figure 7. TEM image of TiO_2 nanoparticles.

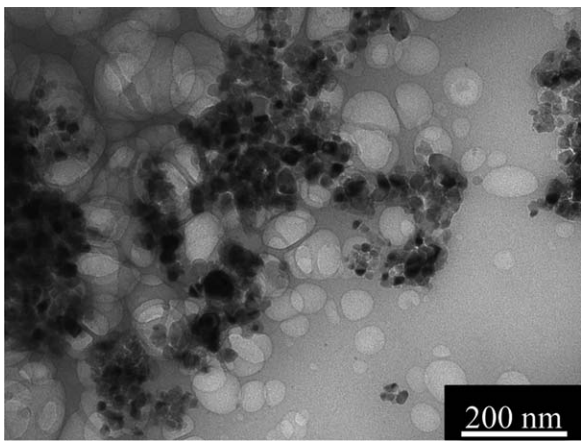

Figure 8. TEM image of TiO_2 with unbonded oligomer.

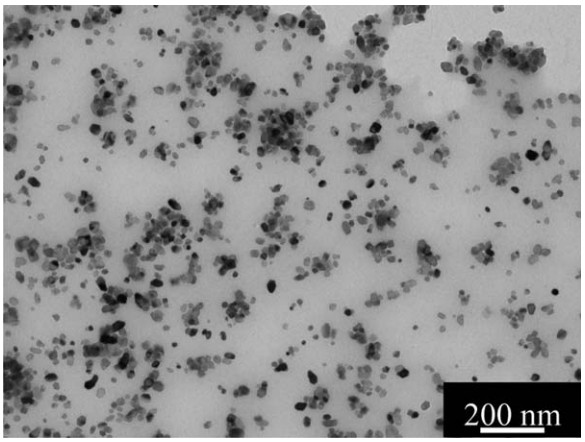

Figure 9. TEM image of TiO_2 with bonded oligomer.

The presence of signals related at —Si—C**H**$_2$(CH$_2$)$_2$NH— or —Si—CH$_2$C**H**$_2$CH$_2$NH— was determined and the corresponding integrals were used as reference values and set as equal to 2, respectively; the integrals of the other signals were evaluated with regard to these values. The integrals of the signals related to the C**H**—OH and to the —C**H**$_2$NH—CO groups were determined for each product, obtaining the DP value. In particular, the following correlations were considered to evaluate DP:

- 2DP = integral of signal related to H-1, H-1′, to H-5, H-5′, to H-2, H-2′, to H-3, H-3′ or to H-4, H-4′, respectively, in the oligotrehaluronamides.
- 2DP = integral of signal related to CH—OH in the oligotartaramides.
- 4DP = integral of signal related to CH$_2$—NHCO (except terminal CH$_2$—NH$_2$).

The signal related to —Si—CH$_2$CH$_2$C**H**$_2$NH—C**H**$_2$—CH$_2$NH— and —C**H**$_2$NH$_2$ (terminal chain) should have integrals equal to 4 for APTMS and 6 for AEAPTMS. In some cases, these integrals appear to be larger than the theoretical values due to the presence of free oligomeric chains in agreement with the simultaneous presence of NC and free oligoamide in the soluble fraction.

Dynamic Light Scattering

To characterize the stability of the water dispersion of TiO_2-polyethylenetartaramide FNPO.1 (1 : 4 : 3), DLS measurements were performed. At the start, after dispersion preparation ($t = 0$), due to the high concentration of particles and the resulting opacity, the dispersion was analyzed using the FOQELS accessory for nondiluted dispersions. The DLS analysis yielded a particle size distribution with the most abundant population ranging between 50 and 125 nm in terms of hydrodynamic diameter (i.e., the size of the diffusing particle, including the polymer coating and the solvation layer) [Figure 6(A)]. A second distribution, related to a much smaller amount of particles, ranged approximately between 350 and 750 nm. During that time, the sedimentation of a small part of the NC particles was observed, leading to the reduction of the opacity of the system. After 24 h, the dispersion was investigated in the conventional geometry (scattering angle of 90°), yielding a particle size distribution ranging between 65 and 100 nm [Figure 6(B)]. A very small amount of larger particles was detected, consistently with a progressive aggregation and sedimentation of particles.

Morphological Analysis

The NC TiO_2-polyethylenetartaramide FNPO.1 (1 : 4 : 3) was analyzed by TEM. A morphological analysis was performed to verify the quality of the dispersion of the NCs. TEM images were compared with those recorded on unmodified TiO_2

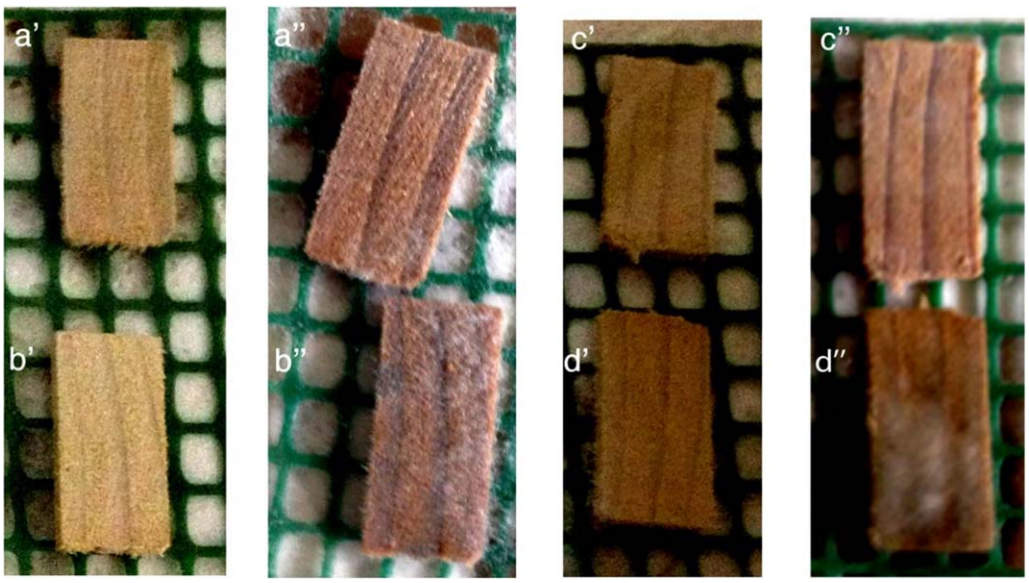

Figure 10. Wood samples with and without NC, kept in the dark or exposed to UV light after three weeks. a′ (time 0) and a″ (time 3 weeks): sample with NC in the dark; b′ (time 0) and b″ (time 3 weeks): sample without NC in the dark; c′ (time 0) and c″ (time 3 weeks): sample with NC in the UV light; d′ (time 0) and d″ (time 3 weeks): sample without NC in the UV light. [Color figure can be viewed in the online issue, which is available at wileyonlinelibrary.com.]

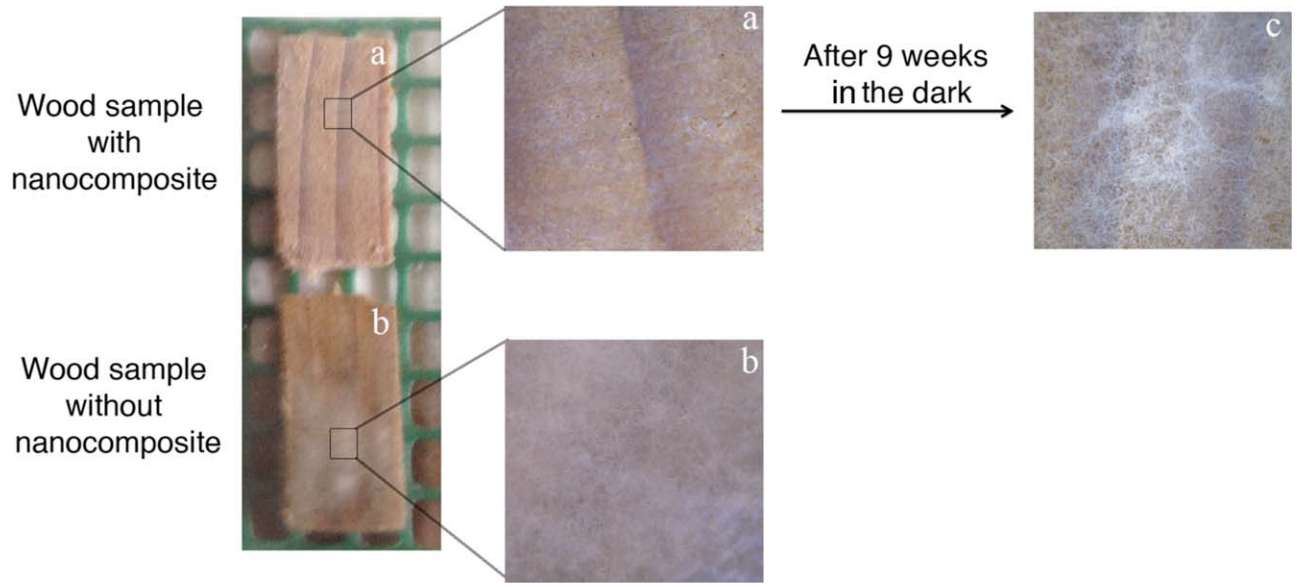

Figure 11. Microscope images (magnification 200×) of wood samples with NC (a) and without NC (b) after UV exposure of 3 weeks; sample with NC after 9 more weeks of incubation in the dark (c). [Color figure can be viewed in the online issue, which is available at wileyonlinelibrary.com.]

and on TiO_2 to which the free polyethylenetartaramide was added.

TEM images of samples containing TiO_2 nanoparticles (Figure 7), TiO_2 with unbonded oligomer (Figure 8), and TiO_2 with bonded oligomer (Figure 9) appear significantly different. In Figure 7, only the presence of the nanoparticles is visible, while in the other images (Figures 8 and 9) the simultaneous presence of oligomer and nanoparticles is shown. Figure 8 reveals the presence of two distinct areas, one constituted of nanoparticles aggregates, the other one with great amount of oligomer; consequently the material does not appear homogeneous. In Figure 9, a better dispersion of nanoparticles in the material is observed in agreement with an improved homogeneity.

Applicative Studies

Photocatalytic Activity of NC Against T. versicolor Attack on F. sylvatica Specimens. Applicative studies on specimens of *F. sylvatica* were performed to demonstrate the antimicrobial effect of a TiO_2-polyethylenetartaramide composite [FNPO.1 (1 : 4 : 3)] against the fungus *T. versicolor* causing white-rot decay.

The samples treated with the NC dispersion (1–8) were observed with a microscope to check the uniformity of the applied film. All samples (1–16) were placed on Petri dishes where *T. versicolor* had previously grown, then half of them were kept in the dark and the remainder was exposed to UV light for 3 weeks.

Both samples incubated in the dark [Figure 10(a′,b′)] exhibited fungal growth with [Figure 10(a″)] or without [Figure 10(b″)] nanoparticles. This result confirms the inactivity of nanoparticles in the dark. Samples exposed to UV light [Figure 10(c′,d′)] only exhibited fungal growth without the NC [Figure 10(d″)]. Accordingly, the activity of the NC was demonstrated when the sample was exposed to UV radiation [Figure 10(c″)].

Optical microscope analysis confirmed fungal growth on the sample without NC [Figure 11(b)] and the absence of any fungal growth in samples containing the NC [Figure 11(a)]. It is interesting to notice how the NC containing samples, on which fungi did not grow during the 3 weeks of UV exposure [Figure 11(a)], showed appearance of fungal growth after 9 more weeks of incubation in the dark [Figure 11(c)]. This confirms the need for exposure to UV radiation to prevent fungal growth.

The UV stability of FNPO.1 NC was studied keeping the product spread on a glass plate exposed to UV light (365 and 254 nm) for 3 weeks while the test with the wood specimens was being carried out. A similar test was performed on the mixture containing TiO_2 nanoparticles and unbonded oligoamide. At the end, products were analyzed with FT-IR (KBr pellet) and ^{1}H-NMR (D_2O solution) spectroscopies. All spectra were comparable to those of the starting material recorded before UV exposure. However, yellowing was observed in the NC probably due to the presence of low amount of oxidation products, which were not detectable in the FT-IR and ^{1}H-NMR spectra. To observe the effect of this yellowing on wood surfaces, new tests were performed on wood specimens. Two new samples (1 and 2) were treated with the NC dispersion, as reported above, and exposed to UV light (365 and 254 nm) for 3 weeks. Colorimetric measurements were realized according to the CIELAB

Table IX. Color Changes after UV Treatments

	After 3 weeks			
Sample	ΔL	Δa	Δb	ΔE
1(exposure at 254 nm)	−1.8	1.0	4.1	4.6
2(exposure at 365 nm)	−2.5	1.8	5.3	6.1

system. The color changes observed on the wood ($\Delta E = 4.6$ at 254 nm and $\Delta E = 6.1$ at 365 nm) were comparable to natural weathering of wood when exposed to ultra-violet light, water, oxygen, or variations in temperature[44] and were hardly noticeable compared to those observed by the human eye after the attack of microorganisms (Table IX).

CONCLUSIONS

Several NCs were synthesized on TiO_2 nanoparticles, allowing oligoamide growth in controlled steps and yielding very homogeneous core-shell systems.

The activated TiO_2 nanoparticles were functionalized using two different coupling agents (obtaining FNP). A preliminary reaction with the diester (obtaining FNPE) was performed to verify the reactivity of FNP and to modify the end group of the FNP as ester group. Polycondensation reactions were carried out in two different synthetic pathways, starting from FNP or from FNPE and using different molar ratios diester/diamine.

The chemical structure of the synthesized products was characterized by ^{1}H-NMR, ^{13}C-NMR and FT-IR. Stable water dispersions were formed with all synthesized NCs. However, soluble and water-insoluble fractions were separated by centrifugation for FT-IR and NMR characterization. Both fractions contained TiO_2 nanoparticles with bonded oligoamides, but the presence of free oligoamide was also observed in the water soluble fractions.

The synthetic procedure has allowed us to obtain composites which are more homogeneous than the blends obtained adding TiO_2 and unbonded oligomer. The results, obtained in the characterization of all products, confirm the possibility of using the same methodologies for several NCs. However, the stability morphological analysis and the antimicrobial activity have been performed only with FNPO as a preliminary study sample.

The morphological analysis showed a homogeneous dispersion when the nanoparticles are bonded with polymer matrix. In fact, the nanoparticles are uniformly distributed without formation of aggregates, which may deteriorate the mechanical properties and reduce the optical transparency of polymer-based NCs.

Applicative tests on wood samples showed the beneficial effect of the NC on wood conservation. Indeed, inhibition of fungal growth was obtained in samples treated with the NC and irradiated UV, as confirmed by microscopical analysis.

ACKNOWLEDGMENTS

The authors thank the Consorzio interuniversitario per lo sviluppo dei Sistemi a Grande Interfase (CSGI) and Dr. Massimo Bonini, Department of Chemistry, University of Florence, for dynamic light scattering measurements and Dr. Marilena Ricci, Department of Chemistry, University of Florence, for colorimetric analyses.

REFERENCES

1. Cipriani, G.; Salvini, A.; Fioravanti, M.; Di Giulio, G.; Malavolti, M. *J. Appl. Polym. Sci.* **2013**, *127*, 420.
2. Oliva, R.; Albanese, F.; Cipriani, G.; Ridi, F.; Giomi, D.; Malavolti, M.; Bernini, L.; Salvini, A. *J. Polym. Res.* **2014**, *21/7*, 1.
3. Morton, D. W.; Kiely, D. E. *J. Appl. Polym. Sci.* **2000**, *77*, 3085.
4. Kiely, D. E.; Smith, T. N. US Patent 131,259 A1, May 21, **2009**.
5. Kiely, D. E.; Chen, L.; Lin, T. H. *J. Polym. Sci. Part A: Polym. Chem.* **2000**, *38*, 594.
6. Kiely, D. E.; Kramer, K.; Zhang, J. WO Patent 052959 A1, June 24, **2004**.
7. Morton, D. W.; Kiely, D. E. *J. Polym. Sci. Part A: Polym. Chem.* **2000**, *38*, 604.
8. Chen, L.; Kiely, D. E. *J. Org. Chem.* **1996**, *61/17*, 5847.
9. Lichtenthaler, F. W. In Biorefineries-Industrial Processes and Products: Status Quo and Future Directions; Kamm, B.; Gruber, P. R.; Kamm, M., Eds.; Wiley-VCH: Weinheim, **2010**; Vol. *2*, Chapter 1, pp 3–59.
10. Kiely, D. E.; Chen, L. US Patent 5,329,044 A, July 12, **1994**.
11. Kubacka, A.; Ferrer, M.; Cerrada, M. L.; Serrano, C.; Sánchez-Chaves, M.; Fernández-García, M.; De Andrés, A.; Jiménez Riobóo, R. J.; Fernández-Martín, F.; Fernández-García, M. *Appl. Catal. B* **2009**, *89*, 441.
12. Fu, G.; Vary, P. S.; Lin, C. T. *J. Phys. Chem. B* **2005**, *109*, 8889.
13. Allen, N. S.; Edge, M.; Verran, J.; Stratton, J.; Maltby, J.; Bygott, C. *Polym. Degrad. Stab.* **2008**, *93*, 1632.
14. Wang, Z.; Li, G.; Peng, H.; Zhang, Z.; Wang, X. *J. Mater. Sci.* **2005**, *40*, 6433.
15. Erkan, A.; Bakir, U.; Karakas, G. *J. Photochem. Photobiol. A Chem.* **2006**, *184*, 313.
16. Martinez-Gutierrez, F.; Olive, P. L.; Banuelos, A.; Orrantia, E.; Nino, N.; Morales Sanchez, E.; Ruiz, F.; Bach, H.; Av-Gay, Y. *Nanomedicine* **2010**, *6*, 681.
17. Foster, H. A.; Ditta, I. B.; Varghese, S.; Steele, A. *Appl. Microbiol. Biotechnol.* **2011**, *90*, 1847.
18. Montazer, M.; Pakdel, E. *J. Photochem. Photobiol. C* **2011**, *12*, 293.
19. Koide, S.; Nonami, T. *Food Control* **2007**, *18*, 1.
20. Long, Q.; Zhao, G. J.; Zheng, B. Z.; Zhou, Y. K. *Yunnan Daxue Xuebao Ziran Kexueban* **2007**, *29/2*, 173.
21. Giannantonio, D. J.; Kurth, J. C.; Kurtis, K. E.; Sobecky, P. A. *Int. Biodeterior. Biodegrad.* **2009**, *63*, 252.
22. Haghighi, F.; Roudbar Mohammdi, S. R.; Mohammdi, P.; Eskandari, M. *Arak Med. Univ. J.* **2012**, *15-1*, 27.
23. Gomez-Ortiz, N.; De la Rosa-Garcia, S.; Gonzalez-Gomez, W.; Soria-Castro, M.; Quintana, P.; Oskam, G.; Ortega-Morales, B. *Appl. Mater. Interfaces* **2013**, *5*, 1556.
24. Othman, S. H.; Abdul Rashid, S.; Mohd Ghazi, T. I.; Abdullah, N. *J. Nanomaterials* **2010**, 512785. DOI: 10.1155/2010/512785.
25. Karvinen, S.; Lamminmaki, R. *J. Solid State Sci.* **2003**, *5*, 1159.
26. Klaine, S. J.; Alvarez, P. J. J.; Batley, G. E.; Fernandes, T. F.; Handy, R. D.; Lyon, D. Y.; Mahendra, S.; Mclaughlin, M. J.; Lead, J. R. *Environ. Toxicol. Chem.* **2008**, *27/9*, 1825.

27. Kwon, S.; Yang, Y. S.; Yang, H. S.; Lee, J.; Kang, M. S.; Lee, B. S.; Lee, K.; Song, C. W. *Toxicol. Res.* **2012**, *28/4*, 217.
28. Xiong, S.; George, S.; Ji, Z.; Lin, S.; Yu, H.; Damoiseaux, R.; France, B.; Ng, K. W.; Loo, S. C. *J. Arch. Toxicol.* **2013**, *87*, 99.
29. Lu, Z.; Wang, J.; Li, Q.; Chen, L.; Chen, S. *Eur. Polym. J.* **2009**, *45*, 1072.
30. Basilissi, L.; Di Silvestro, G.; Farina, H.; Ortenzi, M. A. *J. Appl. Polym. Sci.* **2013**, *128*, 1575.
31. Basilissi, L.; Di Silvestro, G.; Farina, H.; Ortenzi, M. A. *J. Appl. Polym. Sci.* **2013**, *128*, 3057.
32. Von Werne, T.; Patten, T. E. *J. Am. Chem. Soc.* **1999**, *121*, 7409.
33. Bourgeat-Lami, E.; Lang, J. *J. Colloid Interface Sci.* **1998**, *197*, 293.
34. Li, S.; Wang, K.; Zhang, Z.; Song, C.; Cheng, J.; Yang, Z.; Wen, X.; Pi, P. *Sci. China. Chem.* **2010**, *53/3*, 605.
35. Yuvaraj, H.; Park, E. J.; Gal, Y. S.; Lim, K. T. *Colloid Surf. A* **2008**, *313–314*, 300.
36. Haroun, A. A.; Youssef, A. M. *Synth. Met.* **2011**, *161*, 2063.
37. Mallakpour, S.; Barati, A. *J. Polym. Res.* **2012**, *19/2*, 1.
38. Mallakpour, S.; Nikkhoo, E. *J. Polym. Res.* **2013**, *20/2*, 1.
39. Yu, D. G.; An, J. H.; Ahn, S. D.; Kang, S. R.; Suh, K. S. *Colloids Surf. A* **2005**, *266*, 62.
40. Rong, Y.; Chen, H. Z.; Wu, G.; Wang, M. *Mater. Chem. Phys.* **2005**, *91*, 370.
41. Zhao, X.; Zhang, W.; Chen, S.; Zhang, J.; Wang, X. *J. Polym. Res.* **2012**, *19/5*, 1.
42. Suma, K. K.; Jacob, S.; Joseph, R. *Mater. Sci. Eng. B* **2010**, *168*, 254.
43. Peng, X.; Ding, E.; Xue, F. *Appl. Surf. Sci.* **2012**, *258*, 6564.
44. Todaro, L.; D'Auria, M.; Langerame, F.; Salvi, A. M.; Scopa, A. *Surf. Interface Anal.* **2015**, *47/2*, 206.